Machine Learning Non-Markovian Quantum Dynamics

I. A. Luchnikov,[1,2] S. V. Vintskevich,[1] D. A. Grigoriev,[1] and S. N. Filippov[1,3,4]
[1]Moscow Institute of Physics and Technology, Institutskii Pereulok 9, Dolgoprudny, Moscow Region 141700, Russia
[2]Center for Energy Science and Technology, Skolkovo Institute of Science and Technology, 3 Nobel Street, Skolkovo, Moscow Region 121205, Russia
[3]Valiev Institute of Physics and Technology of Russian Academy of Sciences, Nakhimovskii Prospekt 34, Moscow 117218, Russia
[4]Steklov Mathematical Institute of Russian Academy of Sciences, Gubkina Street 8, Moscow 119991, Russia

(Received 27 March 2019; revised manuscript received 28 January 2020; accepted 16 March 2020; published 9 April 2020)

Machine learning methods have proved to be useful for the recognition of patterns in statistical data. The measurement outcomes are intrinsically random in quantum physics, however, they do have a pattern when the measurements are performed successively on an open quantum system. This pattern is due to the system-environment interaction and contains information about the relaxation rates as well as non-Markovian memory effects. Here we develop a method to extract the information about the unknown environment from a series of projective single-shot measurements on the system (without resorting to the process tomography). The method is based on embedding the non-Markovian system dynamics into a Markovian dynamics of the system and the effective reservoir of finite dimension. The generator of Markovian embedding is learned by the maximum likelihood estimation. We verify the method by comparing its prediction with an exactly solvable non-Markovian dynamics. The developed algorithm to learn unknown quantum environments enables one to efficiently control and manipulate quantum systems.

DOI: 10.1103/PhysRevLett.124.140502

Introduction.—Quantum systems are never perfectly isolated which makes the study of open quantum dynamics important for various disciplines including solid-state physics [1], quantum chemistry [2], quantum sensing [3], quantum information transmission [4], and quantum computing [5]. Open quantum dynamics is a result of interaction between the system of interest and its environment. It is usually assumed that the environment is an infinitely large reservoir in statistical equilibrium, which has a well-defined interaction with the system [6]. However, the environments of many physical systems are rather complex and structured [7–19]. A model of the system-environment interaction is often heuristic and oversimplified (e.g., a harmonic environment), but even in this case the analysis is rater complicated and requires some elaborated analytical and numerical methods [20–22]. A theoretical model may also neglect some additional sources of decoherence and relaxation. The experimental analysis of the environmental degrees of freedom is difficult because of their inaccessibility in practice. In fact, one can only get some information about the actual environment by probing the system [23,24]. Therefore, one faces an important problem to learn the *unknown* environment and its interaction with the quantum system by probing and affecting the system only.

This problem can be partly solved within the assumption of fast bath relaxation, when the system density operator ϱ_S experiences the semigroup dynamics $\varrho_S(t) = e^{\mathcal{L}_S t}\varrho_S(0)$ with the Gorini-Kossakowski-Sudarshan-Lindblad (GKSL) generator $\mathcal{L}_S$ [25,26]. In this case, the generator is reconstructed by performing a process tomography of the channel $\Phi_S(t_1) = e^{\mathcal{L}_S t_1}$ for a fixed time $t_1 > 0$ [27,28]. The actual dynamics does not usually reduce to a semigroup though [29–31]. The problem of learning the environment is mostly attributed to memory effects accompanying the non-Markovian dynamics. In this case, one can still resort to the process tomography of channels $\Phi_S(t_1)$, $\Phi_S(t_2)$, …, $\Phi_S(t_K)$ by preparing various initial system states $\varrho_S(0)$ and performing different measurements on the system at time moments $t_1 < t_2 < \cdots < t_K$. This procedure is time consuming because one has to gather enough statistics for all time moments (the total number of required measurements is Kd_S^8/ϵ^2 for a d_S-dimensional quantum system and the accuracy ϵ of statistical reconstruction [32,33]). Moreover, the tomographic reconstruction of each channel $\Phi_S(t_i)$ implies resetting the environment in the same initial state after each measurement, which is difficult to control in the experiment, especially for a strong coupling between the system and environment.

Recently proposed methods exploit the transfer tensor techniques [34–36] to learn the Nakajima-Zwanzig equation [37,38] $(d/dt)\varrho_S(t) = \int_0^t \mathcal{K}(t-t')\varrho_S(t')dt'$ and the recurrent neural networks [39] for defining Lindblad operators and learning the convolutionless master equation $(d/dt)\varrho_S(t) = \mathcal{L}_S(t)\varrho_S(t)$. An implementation of the latter approach in practice encounters the same difficulties related

with the necessity to perform state tomography at different time steps.

In this Letter, we develop a method to learn the effective Markovian embedding [24,40–44] for non-Markovian processes instead of learning the master equation for the system (S). Within such an approach, the environment is effectively divided into two parts: the first one carries memory of the system and is responsible for non-Markovian dynamics [effective reservoir (ER)]; the second one is memoryless and causes Markovian decoherence and dissipation of $S + \mathrm{ER}$. The system evolution reads

$$\varrho_S(t) = \mathrm{tr}_{\mathrm{ER}}[\varrho_{S+\mathrm{ER}}(t)], \tag{1}$$

$$\frac{d\varrho_{S+\mathrm{ER}}(t)}{dt} = \mathcal{L}_{S+\mathrm{ER}}[\varrho_{S+\mathrm{ER}}(t)], \tag{2}$$

where the generator $\mathcal{L}_{S+\mathrm{ER}}$ governs dissipative and decoherence processes on the system and the effective reservoir.

A division of the environment into two parts is similar to the pseudomode method [45–47], the reaction coordinate model [48,49], and the non-Markovian core model [50], where one derives a Markovian master equation in the GKSL form for the extended system comprising the system and a finite number of auxiliary modes. In spin-bosonic models, the Markovian embedding is justified if the bath correlation function has exponentially damped correlations [19]. However, for power-law bath correlation functions with long-range tails [51], the number of auxiliary modes diverges, which limits applicability of the Markovian embedding at a long timescale.

The density operator $\varrho_S(t)$ is unaccessible in a single measurement though, so any relevant information about the system is only gained in a series of measurements. On the other hand, measurement interventions into the system evolution complicate the analysis due to the no-information-without-disturbance principle. Consider a series of projective measurements performed on the system at different times $t_1 < t_2 < \cdots < t_n$, with the measurement basis being chosen randomly, see Fig. 1. The measurement outcomes seem to be completely uninformative due to the intrinsic probabilistic nature of quantum mechanics and the wave function collapse at each measurement, as an example in Fig. 1 suggests. However, such a series of measurement outcomes does contain some information because the outcomes at each time moment are not equiprobable but appear in accordance with the Born rule. In this Letter, we demonstrate that a sufficiently long series of measurement results has a *pattern* that can be recognized by a machine [52]. This is a sharp distinction from conventional tomographic approaches based on numerous repetitions of identical experiments to gather enough statistics.

Our algorithm maximizes the likelihood of observed measurement outcomes and provides the generator $\mathcal{L}_{S+\mathrm{ER}}$ for any fixed dimension of the effective reservoir d_{ER},

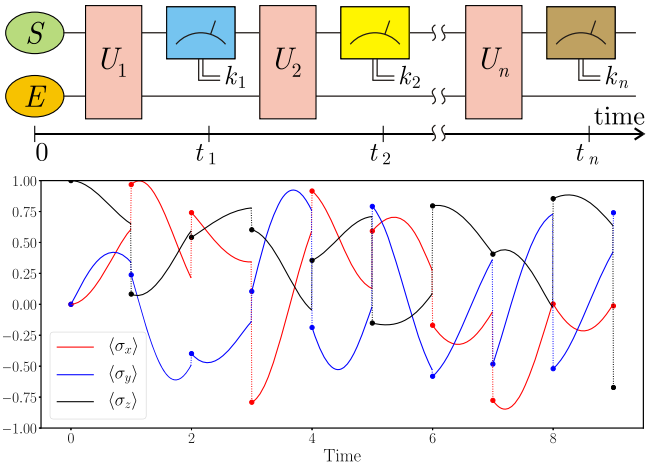

FIG. 1. (Top) Interventions into the open dynamics of the system S by projective measurements. Blocks $\{U_i\}$ depict the interaction between S and the actual environment (E) in between the measurements. (Bottom) Example of the Bloch vector evolution for a qubit system subjected to measurements in random bases at time moments $t_i = i$. Circles correspond to the wave function collapse.

which is a hyperparameter. Computationally, the optimal d_{ER} corresponds to the maximal likelihood on the validation set, which prevents overfitting (see Supplemental Material [53]). Physically, the sufficient value of d_{ER} can be estimated through a reduced set of parameters: the system-environment coupling strength, reservoir correlation time, cutoff frequency of the spectral function, and system's number of degrees of freedom interacting with the environment [44,53]. Alternatively, d_{ER} can also be estimated via the ensemble learning method [61].

If the system evolution is Markovian ($d_{\mathrm{ER}} = 1$), then the result of measurement at time t_k depends on the measurement outcome at time t_{k-1} only and does not depend on results of earlier measurements at times $t_{k-2}, t_{k-3}, \ldots$ [62]. Instead, the non-Markovian dynamics is accompanied by correlations in the measurement outcomes [62–66], which can be analyzed via the process matrix [67] and the process tensor [68]. The process tensor is a particular form of a quantum network [69], which is defined through the generator $\mathcal{L}_{S+\mathrm{ER}}$ in our model, see Fig. 2. The reconstruction of a general process tensor requires exponentially many projective measurements [70]. However, the process tensor has a peculiar form in our model and depends on the generator $\mathcal{L}_{S+\mathrm{ER}}$ only, so it can be reconstructed by maximizing the likelihood of getting the observed outcomes for a single series of measurements without resorting to the full quantum tomography.

Likelihood function and its gradient.—Suppose the experimental setup allows for projective measurements of the system at times $t_i = i\tau$, $i = 1, \ldots, n$, with the measurement basis $\{|\varphi_k^{(i)}\rangle\}_{k=1}^{d_S}$ being randomly chosen at each time moment t_i. Observation of the particular

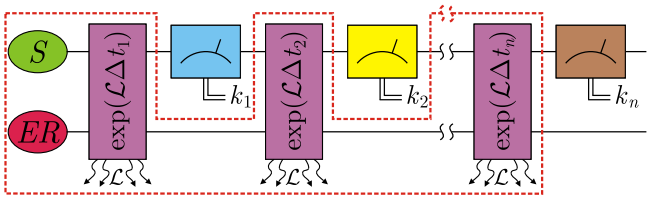

FIG. 2. Markovian embedding of the open dynamics: S and ER experience semigroup dynamics with the generator $\mathcal{L}$; $\Delta t_i = t_i - t_{i-1}$. The process tensor is depicted by the dotted line.

measurement outcome k_i transforms the system state into $|\varphi_{k_i}^{(i)}\rangle\langle\varphi_{k_i}^{(i)}|$. Denote $E_i = |\varphi_{k_i}^{(i)}\rangle\langle\varphi_{k_i}^{(i)}| \otimes I_{\mathrm{ER}}$ the projector acting on the system and effective reservoir. The collection of projectors $\{E_i\}_{i=1}^n$ is the training *dataset* that feeds the learning algorithm.

A superoperator $\Phi = \exp(\tau\mathcal{L}_{S+\mathrm{ER}})$ governs the system and the effective reservoir evolution in between two sequential measurements. The probability to get the particular sequence of measurement outcomes $\{k_i\}_{i=1}^n$ (the data $\{E_i\}_{i=1}^n$) equals [71]

$$p = \mathrm{tr}\{E_n \ldots \Phi[E_1 \Phi(\varrho_{S+\mathrm{ER}}(0))E_1]\ldots E_n\}. \tag{3}$$

The likelihood (3) admits alternative useful forms. Let $\Phi^\dagger$ be dual to Φ [72], then one can split Eq. (3) after mth measurement and get $p = \mathrm{tr}[\tilde{\varrho}_{S+\mathrm{ER}}(t_m)\mathcal{E}_{S+\mathrm{ER}}(t_m)]$, where the recurrence relation $\tilde{\varrho}_{S+\mathrm{ER}}(t_{i+1}) = E_i\Phi[\tilde{\varrho}_{S+\mathrm{ER}}(t_i)]E_i$ with $\tilde{\varrho}_{S+\mathrm{ER}}(0) = \varrho_{S+\mathrm{ER}}(0)$ defines the *forward* propagation of the subnormalized density operator along the tensor network in Fig. 3(a) and the recurrence relation $\mathcal{E}_{S+\mathrm{ER}}(t_{i-1}) = \Phi^\dagger[E_i\mathcal{E}_{S+\mathrm{ER}}(t_i)E_i]$ with $\mathcal{E}_{S+\mathrm{ER}}(t_n) = I_{S+\mathrm{ER}}$ defines the *backward* propagation [73] of effects in the Heisenberg picture along the tensor network in Fig. 3(b). This leads to a "sandwich" formula

$$p = \mathrm{tr}\{\Phi[\tilde{\varrho}_{S+\mathrm{ER}}(t_{m-1})]E_m\mathcal{E}_{S+\mathrm{ER}}(t_m)E_m\}, \tag{4}$$

which is valid for all $m = 1, \ldots, n$, see Fig. 3(c).

The likelihood function is to be maximized over parameters of the generator $\mathcal{L}_{S+\mathrm{ER}}$ defining $\Phi = \exp(\tau\mathcal{L}_{S+\mathrm{ER}})$. Such a maximization is the most common approach in supervised machine learning [74]. The problem is that not every generator $\mathcal{L}_{S+\mathrm{ER}}$ defines a legitimate (completely positive and trace preserving) map Φ. To overcome this obstacle and simplify the implementation of the gradient ascent method [75], we use the Stinespring dilation for the channel Φ [see, e.g., [76] and Fig. 3(c)],

$$\Phi[\varrho_{S+\mathrm{ER}}] = \mathrm{tr}_A[U(H)\varrho_{S+\mathrm{ER}} \otimes \varrho_A U^\dagger(H)], \tag{5}$$

where ϱ_A is a *fixed* pure state of the d_A-dimensional ancilla (A), $d_A = (d_S d_{\mathrm{ER}})^2$, $U(H) = \exp(-iH\tau)$ is a unitary evolution operator, and H is the effective Hamiltonian of $S + \mathrm{ER} + A$. Equation (5) guarantees Φ is completely positive and trace preserving provided H is Hermitian. The ancillary operator ϱ_A plays the role of a renewable subenvironment in quantum collision models [77–79] and the memoryless (Markovian) part of the environment [61].

Because of the Stinespring dilation, the likelihood function is now to be maximized over parameters of the effective Hamiltonian, i.e., matrix elements $H_{\mu\nu} = \langle\mu|H|\nu\rangle$ of H in some computational basis $\{|\mu\rangle\}_{\mu=1}^{d_S d_{\mathrm{ER}} d_A}$. This means that parameters $H_{\mu\nu}$ are iteratively adjusted in the direction of the gradient of the logarithmic likelihood $g_{\mu\nu} = \partial \log p/\partial H_{\mu\nu}$. Since the likelihood function is the n-degree monomial with respect to both operators $U(H)$ and $U^\dagger(H)$, we readily get (see Supplemental Material [53])

$$g_{\mu\nu} = \frac{1}{p}\sum_{m=1}^{n} \mathrm{tr}\Bigg\{[E_m\mathcal{E}_{S+\mathrm{ER}}(t_m)E_m] \otimes I_A \times \left[\frac{\partial U(H)}{\partial H_{\mu\nu}}\tilde{\varrho}_{S+\mathrm{ER}}(t_{m-1}) \otimes \varrho_A U^\dagger(H) + \mathrm{H.c.}\right]\Bigg\}, \tag{6}$$

where the derivative $\partial U(H)/\partial H_{\mu\nu}$ is expressed through the spectral decomposition $H = \sum_k \lambda_k|\psi_k\rangle\langle\psi_k|$ as [53]

$$\frac{\partial U(H)}{\partial H_{\mu\nu}} = \sum_{k,l}\frac{e^{-i\lambda_k\tau} - e^{-i\lambda_l\tau}}{\lambda_k - \lambda_l}\langle\psi_k|\mu\rangle\langle\nu|\psi_l\rangle|\psi_k\rangle\langle\psi_l|. \tag{7}$$

Keeping in a computer memory the operators $\tilde{\varrho}_{S+\mathrm{ER}}(t_i)$ and $\mathcal{E}_{S+\mathrm{ER}}(t_i)$ for forward and backward propagations, respectively, we efficiently calculate the gradient in $O(n)$ steps. Since $\log p$ is a highly nonlinear and nonconvex function with respect to parameters $H_{\mu\nu}$, its optimization is accompanied with overcoming the convergence to local extremums and the slow convergence rate. In what follows, we use techniques that were shown to perform well in such nonconvex optimization problems as neural network learning [80].

Learning algorithm.—The learning algorithm, which estimates the generator $\mathcal{L}_{S+\mathrm{ER}}$ based on the training dataset

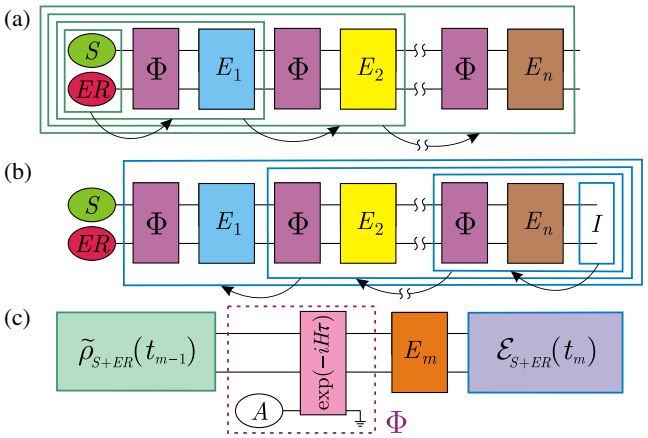

FIG. 3. (a) Forward propagation for subnormalized density operators $\tilde{\varrho}_{S+\mathrm{ER}}(t_i)$. (b) Backward propagation for effects $\mathcal{E}_{S+\mathrm{ER}}(t_i)$. (c) Likelihood functional in Eq. (4) and the Stinespring dilation (5) for Φ (dotted line).

$\{E_i\}_{i=1}^n$, is as follows [81]: (1) Fix the hyperparameter d_{ER}. Initialize the model by randomly choosing the factorized state $\varrho_{S+\mathrm{ER}}(0) = \varrho_S(0) \otimes \varrho_{\mathrm{ER}}(0)$ and the factorized Hamiltonian $H = H_{S+\mathrm{ER}} \otimes I_A$. (2) Calculate the forward-propagation operators $\{\tilde{\varrho}_{S+\mathrm{ER}}(t_i)\}_{i=1}^n$ and the backward-propagation operators $\{\mathcal{E}_{S+\mathrm{ER}}(t_i)\}_{i=0}^{n-1}$. (3) Calculate the likelihood (4). (4) Find the spectral decomposition of the $d_S d_{\mathrm{ER}} d_A$-dimensional operator H and calculate $\partial U(H)/\partial H_{\mu\nu}$ via (7). (5) Estimate the gradient (6) via a batch of summands and results of items 2–4. (6) Feed the estimated gradient to an advanced optimization method (e.g., the adaptive moment estimation algorithm [82]) and get the increment ΔH. (7) Update the Hamiltonian $H \to H + \Delta H$ and repeat items 2–6 until the likelihood converges. (8) Make use of the final update of H to find the channel Φ and the generator $\mathcal{L}_{S+\mathrm{ER}} = (1/\tau) \ln \Phi$.

Synthetic data generation.—We apply the learning algorithm above to the *in silico* training set $\{E_i\}_{i=1}^n$ generated in a non-Markovian composite bipartite collision model[83]. We consider a bipartite system $S + S_1$ composed of the very open qubit system under study S and one auxiliary qubit system S_1. The bipartite system successively interacts with identical subenvironments during some collision time (see Supplemental Material [53]). Such a model is quite rich and describes, e.g., a qubit subject to random telegraph noise. The benefit of this model is that the measurement interventions into the system evolution are explicitly taken into account (see Supplemental Material [53]).

Validation.—We run the learning algorithm for various values of the hyperparameter $d_{\mathrm{ER}} = 1, 2, 4, 6$ on the generated training set $\{E_i\}_{i=1}^n$, $n = 10^5$ [53]. The value $d_{\mathrm{ER}} = 1$ corresponds to the best Markovian approximation for the dynamics that is most compatible with the observed measurement outcomes. However, the likelihood for $d_{\mathrm{ER}} = 1$ is less than that for non-Markovian models with $d_{\mathrm{ER}} \geq 2$, see Fig. 4(a). The greater d_{ER}, the wider the complexity class of possible dynamics [44]. If $d_{\mathrm{ER}} = d_S^n$, then any series of projectors $\{E_i\}_{i=1}^n$ can be perfectly reconstructed with the likelihood $p(\{E_i\}_{i=1}^n) = 1$, which is an ultimate case of overfitting [see Supplemental Material [53] and Fig. 4(b)]. The maximally achieved values of the logarithmic likelihood $\log p(\{E_i\}_{i=1}^n)$ on the training set monotonically increase with the increase of d_{ER}. To avoid overfitting, we calculate the likelihood (3) on a separate *validation set* of projectors $\{E_i\}_{i=n+1}^{2n}$. Figure 4(a) shows that, for the data analyzed, the logarithmic likelihood $\log p(\{E_i\}_{i=n+1}^{2n})$ on the validation set increases up to $d_{\mathrm{ER}} = 2$ and then diminishes. The Markovian embedding with $d_{\mathrm{ER}} = 2$ is the simplest model that is the most compatible with the observed series of measurement outcomes. This is an expected result because we used the synthetic data generated within a collision model with qubits, $d_{S_1} = 2$. For real experimental data, the hyperparameter d_{ER} is tuned in such a way that the likelihood on the validation set achieves its maximum. Tuning is reasonable to perform in the vicinity of the physical estimate for d_{ER} derived in Ref. [44].

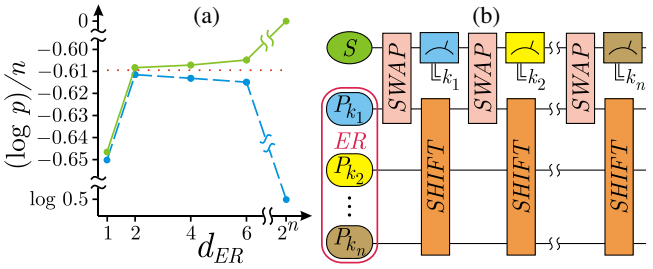

FIG. 4. (a) Logarithmic likelihood per measurement vs dimension of the effective reservoir for the training set $\{E_i\}_{i=1}^n$ (solid line) and the validation set $\{E_i\}_{i=n+1}^{2n}$ (dashed line). Theoretical prediction for the generated data is depicted by a dotted line. (b) Ultimate overfitting with the exponentially big effective reservoir composed of the projectors observed, swap gates, and the shift operator $i \to i-1$, $1 \to n$ for subenvironments.

Results.—With the estimated generator $\mathcal{L}_{S+\mathrm{ER}}$ at hand, we predict the open system dynamics $\varrho_S(t)$ by Eqs. (1) and (2) and compare it with the exact theoretical model (with no measurement interventions). The missing initial state of the effective reservoir is chosen to be the equilibrium state $\mathrm{tr}_S[\varrho^{\infty}_{S+\mathrm{ER}}]$ such that $\mathcal{L}_{S+\mathrm{ER}}[\varrho^{\infty}_{S+\mathrm{ER}}] = 0$. The results are depicted in Fig. 5. Good agreement between the estimated dynamics and the exact one demonstrates that the presented learning algorithm actually extracts useful information from the correlation pattern in a sequence of measurements on the open quantum system.

The quality of the estimated dynamics is assessed in two ways. (i) If the exact dynamics $\Phi_S(t)$ is known, we calculate the distinguishability between the estimated dynamics and the exact one, then average over time moments within the interval $[0, T]$. The result is $\varepsilon = 0.03$ for $T = 50$ (see Supplemental Material [53]). (ii) If the exact solution is not known, the quality of the estimated dynamics is assessed within the variational Bayesian inference approach. This approach yields $\varepsilon = 0.05$ for

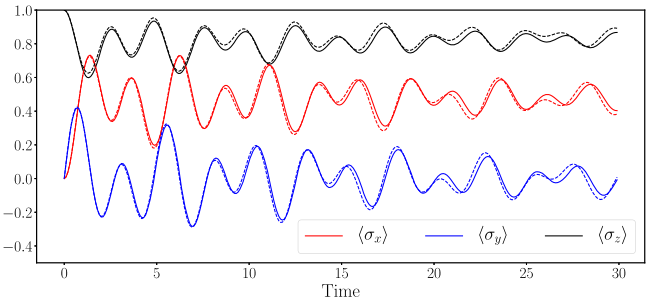

FIG. 5. Bloch vector components $\langle\sigma_i(t)\rangle = \mathrm{tr}[\varrho_S(t)\sigma_i]$ vs dimensionless time for the exact dynamics (solid line) and the learning-based prediction (dotted line).

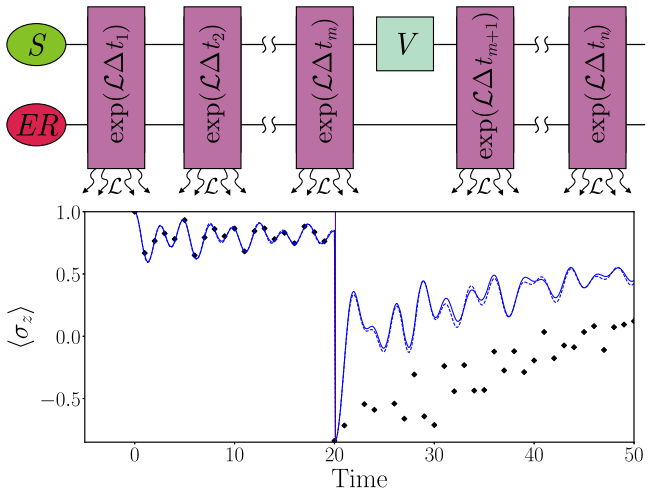

FIG. 6. Compatibility of the process tensor formalism with a coherent control gate V applied to the system (top). Example of non-Markovian qubit dynamics with a quick control gate $V = \sigma_x$ applied at $t' = 20$ (bottom): exact solution (solid line), estimated solution within the Markovian embedding approach (dotted line), solution within the full process tomography approach (dots).

$T = 50$ and the standard deviation 0.025 for matrix elements of the estimated density operator $\varrho_S(T)$ [53].

The average error in estimating the discretized process $\{\Phi_S(t_i)\}_{i=1}^K$ scales as $1/\sqrt{n}$ and is essentially independent of K in the proposed algorithm (see Supplemental Material [53]) because all the channels $\{\exp(\mathcal{L}_{E+\mathrm{ER}}\Delta t_i)\}_{i=1}^K$ in the process tensor in Fig. 1 are defined by a single generator $\mathcal{L}_{S+\mathrm{ER}}$ independent of time moments $\{t_i\}_{i=1}^K$ (parameter sharing). On the other hand, the full process tomography yields the error scaling as $\sqrt{K/n}$ with the same total number of measurements n [53]. Therefore, the proposed method is $\sqrt{K}$ times more efficient as compared to the full process tomography for large K.

Importantly, the formalism of Markovian embedding is compatible with a control operation on system S, say, a quick unitary transformation $\varrho_S(t') \to V\varrho_S(t')V^\dagger$ at time moment t'. After the operation, $\varrho_S(t) = \mathrm{tr}_{\mathrm{ER}}\{\exp[(t-t')\times \mathcal{L}_{S+\mathrm{ER}}]\varrho_{S+\mathrm{ER}}(t')\}$. The result is in good agreement with the exact dynamics (Fig. 6), thus opening an avenue toward efficient control and manipulation of non-Markovian quantum systems. In contrast, the conventional process tomography cannot take such a control operation into account: its prediction $\Phi_S(t)\Phi_S(t')^{-1}[V\varrho_S(t')V^\dagger]$ differs from $\varrho_S(t)$ because of the system-environment correlations [53,84–86], see Fig. 6.

Conclusions.—We proposed a method to learn the Markovian embedding for non-Markovian quantum evolution. The primary information needed is the outcomes of successive projective measurements on the system. Correlations in the measurements at different times indicate non-Markovianity and allow for the reconstruction of memory effects. The decay of correlations between spaced-in-time measurements enables the reconstruction of relaxation effects. Both memory and relaxation phenomena are taken into account by the generator $\mathcal{L}_{S+\mathrm{ER}}$ acting on the system and the effective reservoir of finite dimension. Our algorithm estimates $\mathcal{L}_{S+\mathrm{ER}}$ and does not exploit the full tomography of either states or processes. Learnability of the algorithm is tested on a dataset for the non-Markovian qubit dynamics. The presented approach enables one to take control on the system into consideration, which is impossible with conventional tomographic techniques.

The authors thank Peter Staňo for useful comments. Conceptualization, implementation, and validation of the learning algorithm is supported by the Russian Foundation for Basic Research under Projects No. 18-37-00282 and No. 18-37-20073 and is performed in Moscow Institute of Physics and Technology, Skolkovo Institute of Science and Technology, and Valiev Institute of Physics and Technology of Russian Academy of Sciences, where S. N. F. was partially supported by Program No. 0066-2019-0005 of the Russian Ministry of Science and Higher Education. Synthetic data generation is performed in Moscow Institute of Physics and Technology, where I. A. L. and S. N. F. were partially supported by the Foundation for the Advancement of Theoretical Physics and Mathematics "BASIS" under Grant No. 19-1-2-66-1. The study of the likelihood function and quantum control is supported by the Russian Science Foundation under Project No. 17-11-01388 and is performed in Steklov Mathematical Institute of Russian Academy of Sciences.

[1] S. Takahashi, R. Hanson, J. van Tol, M. S. Sherwin, and D. D. Awschalom, Quenching Spin Decoherence in Diamond Through Spin Bath Polarization, Phys. Rev. Lett. **101**, 047601 (2008).

[2] L. Valkunas, D. Abramavicius, and T. Mancal, *Molecular Excitation Dynamics and Relaxation: Quantum Theory and Spectroscopy* (Wiley, New York, 2013).

[3] C. L. Degen, F. Reinhard, and P. Cappellaro, Quantum sensing, Rev. Mod. Phys. **89**, 035002 (2017).

[4] M. M. Wilde, *Quantum Information Theory* (Cambridge University Press, Cambridge, England, 2017).

[5] M. A. Nielsen and I. L. Chuang, *Quantum Computation and Quantum Information* (Cambridge University Press, Cambridge, England, 2000).

[6] H. Schoeller, Dynamics of open quantum systems, arXiv: 1802.10014.

[7] B.-H. Liu, L. Li, Y.-F. Huang, C.-F. Li, G.-C. Guo, E.-M. Laine, H.-P. Breuer, and J. Piilo, Experimental control of the transition from Markovian to non-Markovian dynamics of open quantum systems, Nat. Phys. **7**, 931 (2011).

[8] C. Navarrete-Benlloch, I. de Vega, D. Porras, and J. I. Cirac, Simulating quantum-optical phenomena with cold atoms in optical lattices, New J. Phys. **13**, 023024 (2011).

[9] J. Ma, Z. Sun, X. Wang, and F. Nori, Entanglement dynamics of two qubits in a common bath, Phys. Rev. A **85**, 062323 (2012).
[10] U. Hoeppe, C. Wolff, J. Küchenmeister, J. Niegemann, M. Drescher, H. Benner, and K. Busch, Direct Observation of Non-Markovian Radiation Dynamics in 3D Bulk Photonic Crystals, Phys. Rev. Lett. **108**, 043603 (2012).
[11] W. L. Yang, J.-H. An, C. Zhang, M. Feng, and C. H. Oh, Preservation of quantum correlation between separated nitrogen-vacancy centers embedded in photonic-crystal cavities, Phys. Rev. A **87**, 022312 (2013).
[12] K. Roy-Choudhury and S. Hughes, Spontaneous emission from a quantum dot in a structured photonic reservoir: Phonon-mediated breakdown of Fermi's golden rule, Optica **2**, 434 (2015).
[13] S. Gröblacher, A. Trubarov, N. Prigge, G. D. Cole, M. Aspelmeyer, and J. Eisert, Observation of non-Markovian micromechanical Brownian motion, Nat. Commun. **6**, 7606 (2015).
[14] A. González-Tudela and J. I. Cirac, Quantum Emitters in Two-Dimensional Structured Reservoirs in the Nonperturbative Regime, Phys. Rev. Lett. **119**, 143602 (2017).
[15] M. Wittemer, G. Clos, H.-P. Breuer, U. Warring, and T. Schaetz, Measurement of quantum memory effects and its fundamental limitations, Phys. Rev. A **97**, 020102(R) (2018).
[16] F. Wang, P.-Y. Hou, Y.-Y. Huang, W.-G. Zhang, X.-L. Ouyang, X. Wang, X.-Z. Huang, H.-L. Zhang, L. He, X.-Y. Chang, and L.-M. Duan, Observation of entanglement sudden death and rebirth by controlling a solid-state spin bath, Phys. Rev. B **98**, 064306 (2018).
[17] S. Peng, X. Xu, K. Xu, P. Huang, P. Wang, X. Kong, X. Rong, F. Shi, C. Duan, and J. Du, Observation of non-Markovianity at room temperature by prolonging entanglement in solids, Sci. Bull. **63**, 336 (2018).
[18] J. F. Haase, P. J. Vetter, T. Unden, A. Smirne, J. Rosskopf, B. Naydenov, A. Stacey, F. Jelezko, M. B. Plenio, and S. F. Huelga, Controllable Non-Markovianity for a Spin Qubit in Diamond, Phys. Rev. Lett. **121**, 060401 (2018).
[19] F. Mascherpa, A. Smirne, A. D. Somoza, P. Fernández-Acebal, S. Donadi, D. Tamascelli, S. F. Huelga, and M. B. Plenio, Optimized auxiliary oscillators for the simulation of general open quantum systems, arXiv:1904.04822.
[20] A. Strathearn, P. Kirton, D. Kilda, J. Keeling, and B. W. Lovett, Efficient non-Markovian quantum dynamics using time-evolving matrix product operators, Nat. Commun. **9**, 3322 (2018).
[21] M. R. Jørgensen and F. A. Pollock, Exploiting the Causal Tensor Network Structure of Quantum Processes to Efficiently Simulate Non-Markovian Path Integrals, Phys. Rev. Lett. **123**, 240602 (2019).
[22] M. V. Altaisky, N. N. Zolnikova, N. E. Kaputkina, V. A. Krylov, Yu. E. Lozovik, and N. S. Dattani, Entanglement in a quantum neural network based on quantum dots, Photonics Nanostruct. Fundam. Appl. **24**, 24 (2017).
[23] M. Bina, F. Grasselli, and M. G. A. Paris, Continuous-variable quantum probes for structured environments, Phys. Rev. A **97**, 012125 (2018).
[24] R. S. Bennink and P. Lougovski, Quantum process identification: A method for characterizing non-Markovian quantum dynamics, New J. Phys. **21**, 083013 (2019).
[25] V. Gorini, A. Kossakowski, and E. C. G. Sudarshan, Completely positive dynamical semigroups of n level systems, J. Math. Phys. (N.Y.) **17**, 821 (1976).
[26] G. Lindblad, On the generators of quantum dynamical semigroups, Commun. Math. Phys. **48**, 119 (1976).
[27] I. L. Chuang and M. A. Nielsen, Prescription for experimental determination of the dynamics of a quantum black box, J. Mod. Opt. **44**, 2455 (1997).
[28] M. Howard, J. Twamley, C. Wittmann, T. Gaebel, F. Jelezko, and J. Wrachtrup, Quantum process tomography and Lindblad estimation of a solid-state qubit, New J. Phys. **8**, 33 (2006).
[29] I. de Vega and D. Alonso, Dynamics of non-Markovian open quantum systems, Rev. Mod. Phys. **89**, 015001 (2017).
[30] L. Li, M. J. W. Hall, and H. M. Wiseman, Concepts of quantum non-Markovianity: A hierarchy, Phys. Rep. **759**, 1 (2018).
[31] S. N. Filippov and D. Chruściński, Time deformations of master equations, Phys. Rev. A **98**, 022123 (2018).
[32] Yu. I. Bogdanov, A. A. Kalinkin, S. P. Kulik, E. V. Moreva, and V. A. Shershulin, Quantum polarization transformations in anisotropic dispersive media, New J. Phys. **15**, 035012 (2013).
[33] J. Haah, A. W. Harrow, Z. Ji, X. Wu, and N. Yu, Sample-optimal tomography of quantum states, IEEE Trans. Inf. Theory **63**, 5628 (2017).
[34] J. Cerrillo and J. Cao, Non-Markovian Dynamical Maps: Numerical Processing of Open Quantum Trajectories, Phys. Rev. Lett. **112**, 110401 (2014).
[35] A. Gelzinis, E. Rybakovas, and L. Valkunas, Applicability of transfer tensor method for open quantum system dynamics, J. Chem. Phys. **147**, 234108 (2017).
[36] F. A. Pollock and K. Modi, Tomographically reconstructed master equations for any open quantum dynamics, Quantum **2**, 76 (2018).
[37] S. Nakajima, On quantum theory of transport phenomena: Steady diffusion, Prog. Theor. Phys. **20**, 948 (1958).
[38] R. Zwanzig, Ensemble method in the theory of irreversibility, J. Chem. Phys. **33**, 1338 (1960).
[39] L. Banchi, E. Grant, A. Rocchetto, and S. Severini, Modelling non-Markovian quantum processes with recurrent neural networks, New J. Phys. **20**, 123030 (2018).
[40] A. A. Budini, Embedding non-Markovian quantum collisional models into bipartite Markovian dynamics, Phys. Rev. A **88**, 032115 (2013).
[41] S. Xue, M. R. James, A. Shabani, V. Ugrinovskii, and I. R. Petersen, Quantum filter for a class of non-Markovian quantum systems, in *54th IEEE Conference on Decision and Control (Osaka, Japan)* (IEEE, New York, 2015), pp. 7096–7100.
[42] S. Xue, T. Nguyen, M. R. James, A. Shabani, V. Ugrinovskii, and I. R. Petersen, Modelling and filtering for non-Markovian quantum systems, arXiv:1704.00986.
[43] S. Campbell, F. Ciccarello, G. M. Palma, and B. Vacchini, System-environment correlations and Markovian embedding of quantum non-Markovian dynamics, Phys. Rev. A **98**, 012142 (2018).
[44] I. A. Luchnikov, S. V. Vintskevich, H. Ouerdane, and S. N. Filippov, Simulation Complexity of Open Quantum

Dynamics: Connection with Tensor Networks, Phys. Rev. Lett. **122**, 160401 (2019).
[45] A. Imamoglu, Stochastic wave-function approach to non-Markovian systems, Phys. Rev. A **50**, 3650 (1994).
[46] B. M. Garraway, Nonperturbative decay of an atomic system in a cavity, Phys. Rev. A **55**, 2290 (1997).
[47] L. Mazzola, S. Maniscalco, J. Piilo, K.-A. Suominen, and B. M. Garraway, Pseudomodes as an effective description of memory: Non-Markovian dynamics of two-state systems in structured reservoirs, Phys. Rev. A **80**, 012104 (2009).
[48] J. Iles-Smith, N. Lambert, and A. Nazir, Environmental dynamics, correlations, and the emergence of noncanonical equilibrium states in open quantum systems, Phys. Rev. A **90**, 032114 (2014).
[49] J. Iles-Smith, A. G. Dijkstra, N. Lambert, and A. Nazir, Energy transfer in structured and unstructured environments: Master equations beyond the Born-Markov approximations, J. Chem. Phys. **144**, 044110 (2016).
[50] D. Tamascelli, A. Smirne, S. F. Huelga, and M. B. Plenio, Nonperturbative Treatment of Non-Markovian Dynamics of Open Quantum Systems, Phys. Rev. Lett. **120**, 030402 (2018).
[51] E. A. Polyakov and A. N. Rubtsov, Dressed quantum trajectories: Novel approach to the non-Markovian dynamics of open quantum systems on a wide time scale, New J. Phys. **21**, 063004 (2019).
[52] G. Carleo, I. Cirac, K. Cranmer, L. Daudet, M. Schuld, N. Tishby, L. Vogt-Maranto, and L. Zdeborová, Machine learning and the physical sciences, Rev. Mod. Phys. **91**, 045002 (2019).
[53] See Supplemental Material at http://link.aps.org/supplemental/10.1103/PhysRevLett.124.140502 for details on the derivation of the likelihood function gradient, details on the learning algorithm (including overfitting and the hyperparameter d_{ER}), details on the data generation, details on the error estimation (including the variational Bayesian inference approach and a comparison with the full process tomography), and details on the coherent control, which includes Refs. [54–60].
[54] S. N. Filippov, G. N. Semin, and A. N. Pechen, Quantum master equations for a system interacting with a quantum gas in the low-density limit and for the semiclassical collision model, Phys. Rev. A **101**, 012114 (2020).
[55] D. Molchanov, A. Ashukha, and D. Vetrov, Variational dropout sparsifies deep neural networks, in *Proceedings of the 34th International Conference on Machine Learning*, edited by D. Precup and Y. W. Teh (PMLR, Cambridge, 2017), Vol. 70, pp. 2498–2507, http://proceedings.mlr.press/v70/molchanov17a.html.
[56] D. P. Kingma and M. Welling, Auto-encoding variational Bayes, in *Proceedings of the 2nd International Conference on Learning Representations (ICLR 2014)*, arXiv:1312.6114.
[57] S. N. Filippov, Quantum mappings and characterization of entangled quantum states, J. Math. Sci. **241**, 210 (2019).
[58] G. C. Knee, E. Bolduc, J. Leach, and E. M. Gauger, Quantum process tomography via completely positive and trace-preserving projection, Phys. Rev. A **98**, 062336 (2018).
[59] E.-M. Laine, J. Piilo, and H.-P. Breuer, Measure for the non-Markovianity of quantum processes, Phys. Rev. A **81**, 062115 (2010).
[60] I. A. Luchnikov, S. V. Vintskevich, D. A. Grigoriev, and S. N. Filippov, Machine learning non-Markovian quantum dynamics, arXiv:1902.07019v2.
[61] S. Shrapnel, F. Costa, and G. Milburn, Quantum Markovianity as a supervised learning task, Int. J. Quantum. Inform. **16**, 1840010 (2018).
[62] G. Lindblad, Non-Markovian quantum stochastic processes and their entropy, Commun. Math. Phys. **65**, 281 (1979).
[63] F. A. Pollock, C. Rodríguez-Rosario, T. Frauenheim, M. Paternostro, and K. Modi, Non-Markovian quantum processes: Complete framework and efficient characterization, Phys. Rev. A **97**, 012127 (2018).
[64] F. A. Pollock, C. Rodríguez-Rosario, T. Frauenheim, M. Paternostro, and K. Modi, Operational Markov Condition for Quantum Processes, Phys. Rev. Lett. **120**, 040405 (2018).
[65] A. A. Budini, Quantum Non-Markovian Processes Break Conditional Past-Future Independence, Phys. Rev. Lett. **121**, 240401 (2018).
[66] P. Taranto, F. A. Pollock, S. Milz, M. Tomamichel, and K. Modi, Quantum Markov Order, Phys. Rev. Lett. **122**, 140401 (2019).
[67] F. Costa and S. Shrapnel, Quantum causal modelling, New J. Phys. **18**, 063032 (2016).
[68] S. Milz, F. A. Pollock, and K. Modi, An introduction to operational quantum dynamics, Open Syst. Inf. Dyn. **24**, 1740016 (2017).
[69] G. Chiribella, G. M. D'Ariano, and P. Perinotti, Theoretical framework for quantum networks, Phys. Rev. A **80**, 022339 (2009).
[70] S. Milz, F. A. Pollock, and K. Modi, Reconstructing non-Markovian quantum dynamics with limited control, Phys. Rev. A **98**, 012108 (2018).
[71] I. A. Luchnikov and S. N. Filippov, Quantum evolution in the stroboscopic limit of repeated measurements, Phys. Rev. A **95**, 022113 (2017).
[72] $\Phi^\dagger$ is dual to Φ if $\mathrm{tr}[X\Phi[Y]] = \mathrm{tr}[\Phi^\dagger[X]Y]$ for all X and Y.
[73] S. Gammelmark, B. Julsgaard, and K. Mølmer, Past Quantum States of a Monitored System, Phys. Rev. Lett. **111**, 160401 (2013).
[74] C. M. Bishop, *Pattern Recognition and Machine Learning* (Springer, New York, 2006).
[75] S. Boyd and L. Vandenberghe, *Convex Optimization* (Cambridge University Press, Cambridge, England, 2004).
[76] A. S. Holevo, *Quantum Systems, Channels, Information: A Mathematical Introduction* (De Gruyter, Berlin, 2012).
[77] J. Rau, Relaxation phenomena in spin and harmonic oscillator systems, Phys. Rev. **129**, 1880 (1963).
[78] V. Scarani, M. Ziman, P. Štelmachovič, N. Gisin, and V. Bužek, Thermalizing Quantum Machines: Dissipation and Entanglement, Phys. Rev. Lett. **88**, 097905 (2002).
[79] S. N. Filippov, J. Piilo, S. Maniscalco, and M. Ziman, Divisibility of quantum dynamical maps and collision models, Phys. Rev. A **96**, 032111 (2017).
[80] P. Jain and P. Kar, Non-convex optimization for machine learning, Found. Trends Mach. Learn. **10**, 142 (2017).

[81] I. A. Luchnikov, S. V. Vintskevich, D. A. Grigoriev, and S. N. Filippov, Machine learning of Markovian embedding for non-Markovian quantum dynamics, GitHub repository (2019), https://github.com/GrigorievDmitry/Machine-learning-of-Markovian-embedding-for-non-Markovian-quantum-dynamics.

[82] D. P. Kingma and J. Ba, Adam: A method for stochastic optimization, arXiv:1412.6980.

[83] S. Lorenzo, F. Ciccarello, and G. M. Palma, Composite quantum collision models, Phys. Rev. A **96**, 032107 (2017).

[84] M. Gessner and H.-P. Breuer, Detecting Nonclassical System-Environment Correlations by Local Operations, Phys. Rev. Lett. **107**, 180402 (2011).

[85] Á. Rivas, S. F. Huelga, and M. B. Plenio, Quantum non-Markovianity: Characterization, quantification and detection, Rep. Prog. Phys. **77**, 094001 (2014).

[86] S. Milz, M. S. Kim, F. A. Pollock, and K. Modi, Completely Positive Divisibility Does Not Mean Markovianity, Phys. Rev. Lett. **123**, 040401 (2019).